Vietnam Journal of Catalysis and Adsorption
Tạp chí xúc tác và hấp phụ Việt Nam

https://jca.edu.vn

Degradation of 4-nitrophenol in wastewater by nickel-iron nanocatalysts

Thanh Thien Co[1,2]*, Ngoc Hai Yen Nguyen[1,2], Thi Ngoc Quynh Tran[1,2], Minh Nguyet Huynh[1,2], Ha Minh Thu Thai[1,2], Thi Bich Phuong Vo[1,2], Thi Yen Nhi Nguyen[1,2]

[1] *University of Science, Ho Chi Minh City, VIETNAM*
[2] *Vietnam National University, Ho Chi Minh City, VIETNAM*
* *Email: ctthien@hcmus.edu.vn*

ARTICLE INFO

Received: 30/03/2024
Accepted: 22/07/2027
Published: 30/12/2024

Keywords:
4-Nitrophenol;
NiFe nanoparticles;
nanocatalyst

ABSTRACT

Nickel-iron (NiFe) nanoparticles supported on activated carbon were synthesized using $NaBH_4$ as a reducing agent and PVP as a stabilizing agent to prevent the nanoparticles from agglomerating or oxidizing. The entire process is carried out under an inert atmosphere to further prevent oxidation and ensure the purity of the NiFe nanoparticles. The physicochemical properties of the resulting NiFe/C samples were analyzed using SEM, TEM, BET, EDX, and XRD techniques. The NiFe nanoparticles, ranging from 3-11 nm, were evenly dispersed on the activated carbon, exhibiting a specific surface area of 850 m^2/g. A complete conversion (100%) of 4-Nitrophenol within a 6-hour reaction period indicates that the catalyst is highly effective. This suggests that the Nickel-Iron (NiFe) nanoparticles supported on activated carbon are performing exceptionally well in the oxidation reaction to detoxify 4-NP. This study provides a comprehensive understanding of the synthesis, structure, composition, and catalytic performance of the NiFe nanocatalyst.

Introduction

Recent, the contamination of water due to industrial wastewater containing organic pollutants poses a significant threat to the ecological environment [1–3]. Conventional methods for treating organic pollutants, such as flocculation, adsorption, and microbial degradation, are not highly effective [2]. Meanwhile, nanomaterials exhibit unique catalytic properties that accelerate various types of reactions at significantly faster rates, attributed to their elevated surface energies. [4, 5]. Metal nanoparticles have garnered considerable attention from researchers for their versatile applications, including use as catalysts, sensors, antibacterial agents, and in the development of flexible and transparent electrodes [6]. Metal-based nanoparticles possess distinctive characteristics such as abundant vacant sites and large surface area, making them extensively utilized for the removal of a wide range of toxic substances[6, 7]. From this, it promises to bring potential applications as a catalyst in reactions to treat organic pollutants.

4-NP (4-nitrophenol) is commonly employed as an intermediate in the manufacturing processes of pharmaceuticals, pesticides, and dyes [8–10]. In addition, 4-NP is primarily generated during chemical processing activities such as petrochemical manufacturing, rubber synthesis, wood preservation, pesticide production, plastics manufacturing, and paint formulation [3, 11]. Therefore, 4-NP is prevalent in industrial and agricultural

https://doi.org/10.62239/jca.2024.077

wastewaters as a harmful organic pollutant [12]. As a result, it is inevitably released into the environment, leading to contamination [8]. Several methods have been studied for oxidation of 4-NP, including catabolism [13], photocatalytic degradation [13–15], Fenton [16] and electrochemical methods [17–19]. This also serves as the premise for the research idea of this study.

When synthesizing metal nano catalysts, the carrier plays an extremely important role in determining the activity of the catalyst. Activated carbon serves as a critical support in the catalytic industry due to its high specific surface area and stability under acidic/basic conditions, as well as at moderate to high temperatures in low oxidizing atmospheres [20]. Furthermore, its adaptable porous structure and cost-effectiveness render activated carbon suitable for numerous catalytic applications, particularly in liquid-phase reactions[20].

Based on the above facts, this study was conducted with the purpose of synthesizing a type of nano metal catalyst using two main metals, Ni and Fe, on activated carbon as a carrier, with the aim of treating 4-NP pollution and applying it in practical technology.

Experimental

All the chemicals were used as received without further purification. Nickel chloride hexahydrate 99% ($NiCl_2.6H_2O$), iron (II) sulfate heptahydrate 99% $FeSO_4.7H_2O$, sodium hydroxide 98% (NaOH), hydrochloric acid 98% (HCl), hydrogen peroxide 30% (H_2O_2) were purchased from Xilong (China). Sodium borohydride 99% ($NaBH_4$) and 4- Nitrophenol were purchased from Acros Organics (USA). Polyvinyl pyrrolidone K-30 (PVP) were purchased from HiMedia (India). Activated carbon was purchased in Vietnam. Ethanol (C_2H_5OH) was supplied by Chemsol (Vietnam).

The elemental composition of NiFe/C were determined by Energy Dispersive X-Ray Spectroscopy (EDX), performed on EDX 7593-H (Horiba, England). The X-ray diffraction (XRD) patterns were recorded on a PANalytical Empyrean X-ray Diffractometer using CuKα radiation (40 kV, 100 mA, 0.1541 nm). The diffractograms were recorded within the 2θ range 5–80° with a step size of 0.026°. Transmission electron microscopy (TEM) images were collected on JEM-2100 to determine the shape and size of nanoparticles. The morphology was examined by scanning electron microscopy (SEM) recorded on Hitachi S-4800 (HI-9039-0006). The surface area, pore diameter and pore volume of the activated carbon were measured on a Quantachrome Instruments version 11.0.

The NiFe/C catalyst was synthesized according to the following procedure. First, completely dissolve 2.0261 g of polyvinylpyrrolidone (PVP) in a 250 mL two-neck round-bottom flask containing 10 mL of ethanol and 40 mL of deionized water (DI), stir continuously for 30 minutes. Next, add 3 mmol of $NiCl_2.6H_2O$ and 3 mmol of $FeSO_4.7H_2O$ into the flask, stir under nitrogen atmosphere for 1 hour. Gradually add 10 mL of a 1.5 M $NaBH_4$ solution dropwise to the system while maintaining vigorous and continuous stirring, until the solution undergoes a transition to a black colloidal suspension. 3 g of activated carbon were introduced into the flask and stirred at room temperature for 12 hours. After washing to pH 7, the sample was centrifuged and vacuum-dried at 100°C for 16 hours.

The catalytic activity of the NiFe/C sample was evaluated based on the variation in 4-NP concentration during the reaction using HPLC-DAD. The reaction mixture comprised 20 ml of 4-NP solution (50 ppm), a pre-determined amount of NiFe/C catalyst, and 5 ml of H_2O_2 30%. Factors affecting reaction efficiency, including pH (3, 5, 7, 9, 11, adjusted by HCl 10% and NaOH 0.1 N), temperature (30, 60, 90, and 120 °C, refluxed at these temperatures), catalyst percentage (2, 5, 10, and 20%, ratio of the weight of the catalyst to the weight of 4-NP), and reaction time (30, 60, 90, 120, 180, and 360 minutes, recorded the time starting from the addition of H_2O_2), were all investigated.

Results and discussion

The EDX results indicate that iron (Fe) constitutes 3.02% while Nickel (Ni) constitutes 2.27% of the synthesized sample. This demonstrates the presence of these two important metals in the sample, as well as attests to the efficacy of the catalyst impregnation process.

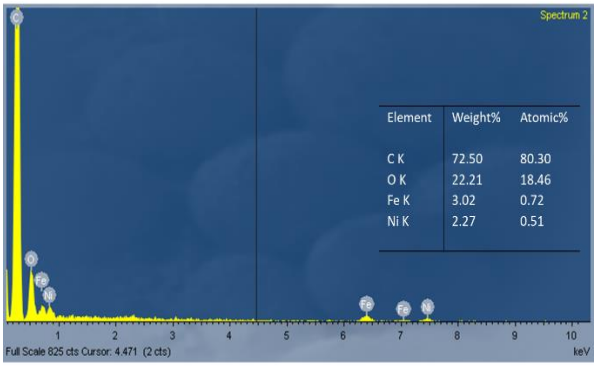

Fig. 1: EDX spectrum of NiFe/C

https://doi.org/10.62239/jca.2024.077

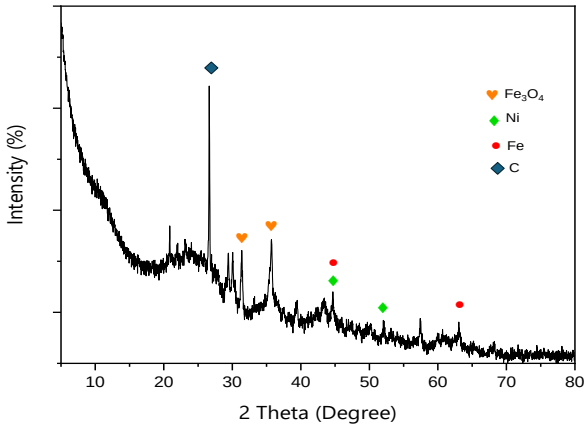

Fig. 2: XRD patterns of NiFe/C

As shown in Figure 2, the NiFe/C catalyst was characterized by XRD method, in which the presence of characteristic diffraction peak of activated carbon is at 2θ of 26.62° and peaks of Ni nanoparticles are at 2θ of 44.67°, 52.05°. Meanwhile, the 2θ values of Fe nanoparticles are at 44.67° and 63.05°. Beside of the existence of metal nanoparticles, there are peaks of iron oxide at 2θ of 31.38° and 35.71°, which could be explained by the oxidation of iron particles to iron oxides due to the exposure to the oxygen gas in the air.

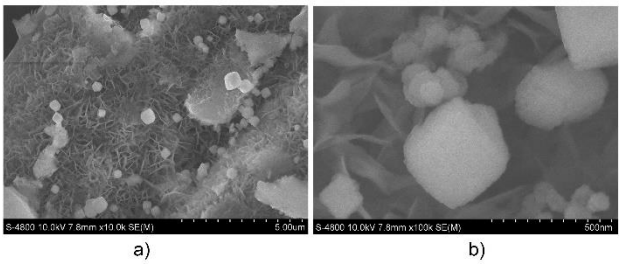

Fig. 3: SEM images of NiFe/C

The SEM analysis reveals that the catalyst samples exhibit a surface structure characterized by numerous pores and an uneven, rugged texture. This configuration enhances the catalyst's surface area, facilitating the dispersion of active sites within the carrier material and increasing the contact area between 4-NP and the catalyst. As a result, this leads to improved efficiency in the treatment process of 4-NP.

The TEM image depicted in Figure 4 illustrates the existence of spherical particles ranging from 3 nm to 11 nm in diameter, with an average size of 6 nm. Through the particle size distribution chart along with TEM images, the nanoparticles are relatively uniform in size and well dispersed. From this, it is evident that the activated carbon has provided a rough and porous surface, allowing the nanoparticles enough space to disperse, with no significant aggregation observed.

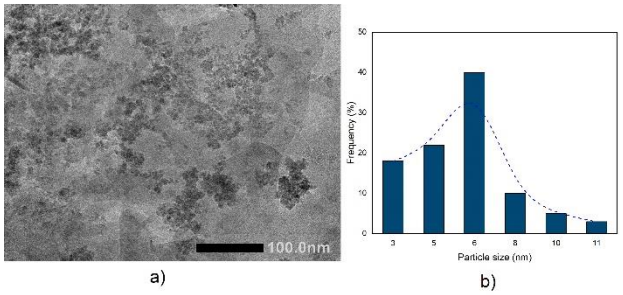

Fig. 4: a) TEM image of NiFe/C b) Particle size distribution of NiFe/C

The specific surface area of the catalyst, as calculated using the Langmuir model, is 850.168 m^2/g, while the BET model yields a value of 617.764 m^2/g. Consequently The catalyst sample has a relatively large surface area, offering the potential for good catalytic efficiency due to excellent adsorption processes as well as the large contact area between 4-NP and the metal centers.

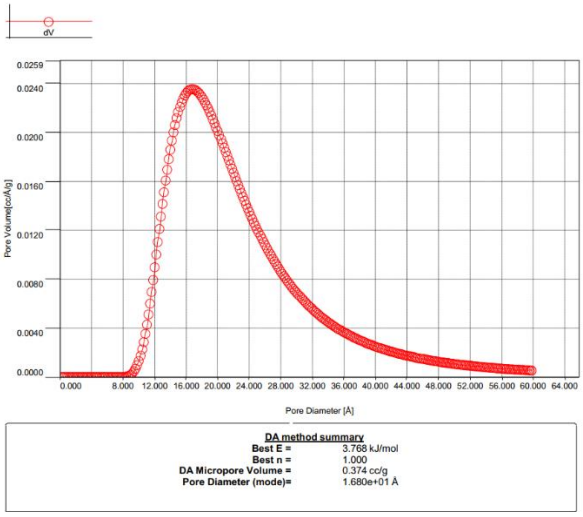

Fig. 5: Pore Size Distribution Desorption

The NiFe/C catalyst exhibits a pore size distribution ranging from 8 Å to 60 Å, with a concentration of pore sizes centered around 16-17 Å as shown on Fig. 5. This suggests that the catalyst sample contains pores of both mesoporous and microporous dimensions.

During the investigation of the catalytic activity of NiFe/C, the oxidation of 4-NP was carried out at various pH values (3, 5, 7, 9, 11). Fig. 6a shows that the conversion gradually increases from pH 3 to pH 7 and then decreases in an alkaline condition. In an alkaline condition, 4-NP generates phenolate salts, thereby impeding the efficiency of the treatment compared to a neutral environment. Conversely, in an acidic condition, metal nanoparticles are unstable due to their reaction with acid, consequently decreasing catalytic activity. Whereas, the efficiency peaks at neutral environment (H=20.3%). Based

https://doi.org/10.62239/jca.2024.077

on these findings, the reaction environment for subsequent investigations has been established.

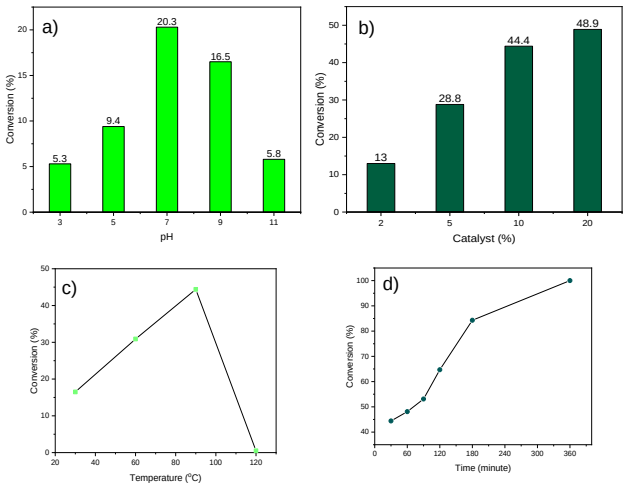

Fig. 6: The impact of various factors on conversion of 4-NP using NiFe/C: a) pH; b) Catalyst percentage; c) Temperature; d) Time.

Following that, the reactions were carried out utilizing different percentages of catalyst to determine the optimal catalyst loading for studying the effects of temperature and reaction time on reaction efficiency. As depicted in Fig. 6b, the conversion rate shows a gradual increase with rising catalyst percentage. Certainly, when the catalyst loading increases, the number of active sites on the catalyst and its adsorption capacity also enhance. Consequently, the oxidation process proceeds more effectively, leading to a faster reduction in the amount of 4-NP. As a result, the overall efficiency increases. In addition, the disparity in conversion rate between using 10% and 20% catalyst is insignificant, 10% catalyst was selected for further exploration in the subsequent two investigations.

Fig. 6c illustrates that during the temperature increase phase from 30 °C to 90 °C, the conversion rate progressively rises, specifically to 16.5% at 30 °C, 30.9% at 60 °C, and 44.4% at 90 °C. However, upon reaching 120 °C, the conversion drops to 0.5%, which is significantly low. This could be due to the excessively high temperature causing the decomposition of H_2O_2 before it can react with 4-NP. Additionally, the high temperature accelerates the desorption process. Consequently, the oxidation reaction occurs ineffectively. Finally, the investigation of the variation in the concentration of 4-NP over time in the oxidation reaction using H_2O_2 in the presence of NiFe/C as a catalyst was also conducted based on previous studies. Therefore, the amount of catalyst chosen for the study was 10% relative to the substrate and reaction was carried out at 90°C. According to the results obtained, which are detailed in Figure 6d, the conversion rate increases progressively with reaction time. After just 90 minutes, a conversion of 53.1% was achieved, and 84.3% was achieved at 180 minutes. The reaction eliminates 4-NP after 360 minutes of reaction. This fully demonstrates the catalytic capability and potential application of NiFe/C in practice.

Conclusion

NiFe nanocatalysts supported on activated carbon was successfully synthesized using the chemical reduction method with $NaBH_4$ as the reducing agent. The physicochemical properties are fully presented in the report. Moreover, the resulting catalyst demonstrates high activity in the oxidation of 4-NP. Notably, under neutral conditions at 90°C, with the nano NiFe catalyst concentration at 10% relative to 4-Nitrophenol, conversion efficiencies exceeding 80% are achieved within 3 hours of reaction.

Acknowledgments

This research is funded by Vietnam National University Ho Chi Minh City (VNU-HCM) under grant number B2023-18-03.

References

1. Zhang, X.; Shi, Z.; Liu, H.; Niu, Y. Inorg Chem Commun 156 (2023) 111219. https://doi.org/10.1016/j.inoche.2023.111219
2. Wang, K.; Ma, J.; Yao, Z.; Zhang, W.; Komarneni, S., Ceram Int 42 (14) (2016) 15981–15988. https://doi.org/10.1016/j.ceramint.2016.07.103
3. Samuel, M. S.; Bhattacharya, J.; Parthiban, C.; Viswanathan, G.; Pradeep Singh, N. D., Ultrason Sonochem 49 (2018) 215–221. https://doi.org/10.1016/j.ultsonch.2018.08.004
4. Mehmood, S.; Janjua, N. K.; Saira, F.; Fenniri, H., Journal of Spectroscopy 2016 (2016). https://doi.org/10.1155/2016/6210794
5. Mahmoud, M. A.; Narayanan, R.; El-Sayed, M. A., Acc Chem Res 46(8) (2013) 1795–1805. https://doi.org/10.1021/ar3002359
6. Hashimi, A. S.; Nohan, M. A. N. M.; Chin, S. X.; Zakaria, S.; Chia, C. H., Nanomaterials 9(7) (2019) 936 https://doi.org/10.3390/nano9070936
7. Das, J.; Velusamy, P., J Taiwan Inst Chem Eng 45(5) (2014) 2280–2285. https://doi.org/10.1016/j.jtice.2014.04.005.
8. Ding, Q.; Kang, Z.; Cao, L.; Lin, M.; Lin, H.; Yang, D. P., Appl Surf Sci 510 (2020) 145526. https://doi.org/10.1016/j.apsusc.2020.145526

9. Gao, D.; Li, S.; Wang, X.; Xi, L.; Lange, K. M.; Ma, X.; Lv, Y.; Yang, S.; Zhao, K.; Loussala, H. M.; Duan, A.; Zhang, X.; Chen, G., J Catal 370 (2019) 385–403. https://doi.org/10.1016/j.jcat.2019.01.011
10. Serrà, A.; Artal, R.; Pozo, M.; Garcia-Amorós, J.; Gómez, E., Catalysts 10(4) (2020) 458 https://doi.org/10.3390/catal10040458
11. Chen, Y.; Sun, F.; Huang, Z.; Chen, H.; Zhuang, Z.; Pan, Z.; Long, J.; Gu, F., Appl Catal B 215 (2017) 8–17. https://doi.org/10.1016/j.apcatb.2017.03.082
12. Lu, Y.; Wan, X.; Li, L.; Sun, P.; Liu, G., Journal of Materials Research and Technology 12 (2021) 1832–1843. https://doi.org/10.1016/j.jmrt.2021.03.093
13. Jun Min, Jun-Jie Zhang, Ning-Yi Zhou, Appl Environ Microbiol 80(19) (2014) 6212–6222. https://doi.org/10.1128/AEM.02093-14
14. Wang, J. C.; Li, Y.; Li, H.; Cui, Z. H.; Hou, Y.; Shi, W.; Jiang, K.; Qu, L.; Zhang, Y. P. A, J Hazard Mater 379 (2019) 120806. https://doi.org/10.1016/j.jhazmat.2019.120806
15. Serrà, A.; Artal, R.; García-Amorós, J.; Sepúlveda, B.; Gómez, E.; Nogués, J.; Philippe, L., Advanced Science 7(3) (2020) 1902447. https://doi.org/10.1002/advs.201902447
16. J. Kiwi, C. Pulgarin, P. Peringer, Applied Catalysis B: Environmental 3(4) (1994) 335–350. https://doi.org/10.1016/0926-3373(94)00008-5
17. Xie, F.; Xu, Y.; Xia, K.; Jia, C.; Zhang, P. Ultrason Sonochem 28 (2016) 199–206. https://doi.org/10.1016/j.ultsonch.2015.07.011
18. Serrà, A.; Alcobé, X.; Sort, J.; Nogués, J.; Vallés, E., J Mater Chem A Mater 4(40) (2016) 15676–15687. https://doi.org/10.1039/c6ta07149j
19. Chen, G. Sep Purif Technol 38(1) (2004) 11–41. https://doi.org/10.1016/j.seppur.2003.10.006
20. Rodríguez Molina, H.; Santos Muñoz, J. L.; Domínguez Leal, M. I.; Reina, T. R.; Ivanova, S.; Centeno Gallego, M. Á.; Odriozola, J. A., Front Chem 7 (2019) https://doi.org/10.3389/fchem.2019.00548